

The Pan-Pacific Planet Search III: Five companions orbiting giant stars

R.A. Wittenmyer^{1*}, R.P. Butler², L. Wang³, C. Bergmann⁴, G.S. Salter⁵,
C.G. Tinney¹, and J.A. Johnson⁶

¹*School of Physics, University of New South Wales, Sydney 2052, Australia*

²*Department of Terrestrial Magnetism, Carnegie Institution of Washington, 5241 Broad Branch Road, NW, Washington, DC 20015-1305, USA*

³*Key Laboratory of Optical Astronomy, National Astronomical Observatories, Chinese Academy of Sciences, A20 Datun Road, Chaoyang District, Beijing, China*

⁴*University of Canterbury, Department of Physics and Astronomy, Christchurch 8041, New Zealand*

⁵*Aix Marseille Université, CNRS, LAM (Laboratoire d'Astrophysique de Marseille) UMR 7326, 13388, Marseille, France*

⁶*Harvard-Smithsonian Center for Astrophysics, Cambridge, MA 02138 USA*

Accepted Received ; in original form

ABSTRACT

We report a new giant planet orbiting the K giant HD 155233, as well as four stellar-mass companions from the Pan-Pacific Planet Search, a southern hemisphere radial velocity survey for planets orbiting nearby giants and subgiants. We also present updated velocities and a refined orbit for HD 47205b (7 CMa b), the first planet discovered by this survey. HD 155233b has a period of 885 ± 63 days, eccentricity $e = 0.03 \pm 0.20$, and $m \sin i = 2.0 \pm 0.5 M_{\text{Jup}}$. The stellar-mass companions range in $m \sin i$ from $0.066 M_{\odot}$ to $0.33 M_{\odot}$. Whilst HD 104358B falls slightly below the traditional $0.08 M_{\odot}$ hydrogen-burning mass limit, and is hence a brown dwarf candidate, we estimate only a 50% *a priori* probability of a truly substellar mass.

Key words:

planetary systems, stars: giants, techniques: radial velocity

1 INTRODUCTION

Radial velocity planet search efforts have been underway for more than 20 years, discovering hundreds of new planetary companions. However, brown-dwarf and stellar-mass companions tend to be largely ignored in these surveys: limited telescope time means that targets showing large-amplitude variations ($\gtrsim 500 \text{ m s}^{-1}$) are usually dropped from the observing queue. Only limited results on such massive companions have been published (Patel et al. 2007), with many objects featuring incomplete orbits. However, such objects remain valuable for exploring the lower end of the mass function and the properties of stellar systems in the Solar neighbourhood. The observed deficit of companions between $13\text{--}80 M_{\text{Jup}}$ is known as the “brown dwarf desert” (Marcy & Butler 2000; Mazeh et al. 2003), and became evident in the earliest days of radial velocity planet searches (Campbell et al. 1988; Murdoch et al. 1993). A comprehensive, self-consistent study by Grether & Lineweaver (2006) confirmed the presence of a “valley” in the brown-dwarf mass range at $M = 31_{-18}^{+25} M_{\text{Jup}}$. Stellar companions are also not to be ignored, since any binary system with a well-

characterised orbit is useful for a range of follow-up science. Most obviously, a precisely-determined binary orbit permits the search for additional Doppler velocity signals due to planets orbiting one or both stars. Binary systems compose $\sim 50\%$ of nearby star systems (Duquennoy & Mayor 1991; Raghavan et al. 2010), yet are hosts to only $\sim 5\%$ of known extrasolar planets. The mechanisms and outcomes of planet formation in close binary systems remain significant questions virtually unexplored by observations.

At the 3.9m Anglo-Australian Telescope (AAT), we carried out a 5-year survey for planets orbiting intermediate-mass evolved stars in an effort to characterise the dependence of planetary system properties on stellar mass (Wittenmyer et al. 2011; Reffert et al. 2015). **The initial sample was selected according to these criteria: $1.0 < (B - V) < 1.2$, $1.8 < M_V < 3.0$, and $V < 8.0$. Of those stars meeting these criteria, 18 were discarded as binaries by their *Hipparcos* multiple systems flag.** From the 167-star Pan-Pacific Planet Search (PPPS) sample, 17 targets turned out to be double-lined spectroscopic binaries (SB2s – Table 1). Since the Doppler velocity technique used here assumes only a single set of spectral lines, we were unable to derive velocities for these binaries and they were dropped from the program as soon as they were identified as

* E-mail: rob@unsw.edu.au (RW)

such. We note that it has recently become possible to modify planet-search Doppler codes to obtain precise velocities for SB2s, by including the secondary star’s spectrum in the modelling process if the flux ratio is known. This novel approach is now being applied to the Alpha Centauri binary system (Bergmann et al. 2015; Endl et al. 2015).

A further 31 stars in the PPPS sample show large-amplitude velocity variations or long-term trends, which indicate stellar-mass companions. This yields a first-order binary fraction of $48/167=29\%$, for a sample which was initially selected to avoid suspected binaries (Wittenmyer et al. 2011). As is common in planet-search programs, these stars were deprecated in observing priority and so the orbits of these massive companions cannot be constrained. However, four stars host shorter-period companions and received enough observations to reliably determine the orbital solutions. Here, we present the velocity data and orbital solutions for stellar-mass companions orbiting HD 34851, HD 94386, HD 104358, and HD 188981. We also present new data and a refined orbital solution for the giant planet orbiting 7 Cma (HD 47205). Section 2 briefly describes the observational data and gives the stellar parameters. In Section 3, we describe the orbit-fitting process. Section 4 gives the companion parameters and our conclusions.

2 AAT OBSERVATIONS AND STELLAR PROPERTIES

The PPPS used the UCLES echelle spectrograph (Diego et al. 1991) at the AAT to obtain high-resolution spectra, with an observing procedure identical to that used by the 16-year Anglo-Australian Planet Search (AAPS). UCLES uses a 1-arcsecond slit to deliver a resolving power of $R \sim 45,000$. An iodine absorption cell, temperature-controlled at $60.0 \pm 0.1^\circ\text{C}$, is placed in the light path. The iodine cell imprints a forest of narrow absorption lines from 5000 to 6200 Å, allowing simultaneous calibration of instrumental drifts as well as a precise wavelength reference (Valenti et al. 1995; Butler et al. 1996). Precise Doppler velocities are derived using the well-established PSF modelling techniques described in Butler et al. (1996). The result is a velocity with a zero-point relative to the stellar template: a high S/N spectrum obtained without the iodine cell at $R \sim 60,000$. The internal uncertainty estimate includes the effects of photon-counting uncertainties, residual errors in the spectrograph PSF model, and variation in the underlying spectrum between the iodine-free template and epoch spectra observed through the iodine cell. A summary of the observations is given in Table 2, and the radial velocities are given in Tables 3–8.

For each new star discussed in this work, we have used our iodine-free template spectrum ($R \sim 60,000$, $S/N \sim 150\text{--}250$) to derive spectroscopic stellar parameters. The same techniques were used in Wittenmyer et al. (2011) and Wittenmyer et al. (2015) for HD 47205 and HD 121056, respectively. In brief, the iron abundance $[\text{Fe}/\text{H}]$ was determined from the equivalent widths of ~ 30 unblended Fe lines, and the LTE model atmospheres adopted in this work were interpolated from the ODFNEW grid of ATLAS9 (Castelli & Kurucz 2004). The effective temperature

(T_{eff}) and bolometric correction (BC) were derived from the colour index $B - V$ and the estimated metallicity using the empirical calibration of Alonso et al. (1999, 2001). Since the colour- T_{eff} method is not extinction-free, we corrected for reddening using $E(B - V)$ (Schlegel et al. 1998). The stellar mass and age were estimated from the interpolation of Yonsei-Yale (Y^2) stellar evolution tracks (Yi et al. 2003). The resulting stellar masses were adopted for calculating the planet masses. Complete stellar parameters from this analysis are given in Table 9.

3 ORBIT FITTING AND COMPANION PARAMETERS

As shown in Table 2, many of the stars considered here received fewer observations than is typical or desired for planet-search efforts. However, the signals in our data are large enough as to be unambiguous, particularly for the stellar-mass companions. We first used a genetic algorithm to search a wide range of orbital periods, running for 10,000 iterations (about 10^6 possible configurations). This approach has been used in our previous work on systems for which data are sparse and/or poorly sampled (e.g. Tinney et al. 2011; Wittenmyer et al. 2011, 2015). In all cases, convergence occurred rapidly, a hallmark of a genuine signal. Again as in our previous work, we then used the best solution from the genetic algorithm as a starting point for the generalized least-squares program *GaussFit* (Jefferys et al. 1988), here used to solve a Keplerian radial velocity orbit model. Finally, we estimated the parameter uncertainties using the bootstrap routine within *Systemic 2* (Meschiarri et al. 2009) on 10,000 synthetic data set realisations. The results are given in Table 10.

4 RESULTS

We have continued to observe HD 47205 in the four years since the discovery of HD 47205b (Wittenmyer et al. 2011). **We have added 6 new epochs, extending the baseline by 964 days, a factor of two longer than reported in the discovery work.** The updated orbital solution given in Table 10 is significantly more precise, and has an rms of only 6.5 m s^{-1} , further strengthening the case for the planet’s presence and apparent solitude. **Notably, the orbital period is now slightly longer (796d compared to 763d); other parameters remain within 1σ of their originally-reported values.** No residual trends or periodicities are evident, though of course very low-mass planets could remain undetected with our radial velocity precision and cadence (e.g. Wittenmyer et al. 2009b; Swift 2015).

4.1 A giant planet orbiting HD 155233

We have obtained 21 radial velocity measurements of HD 155233, indicating a linear trend and a periodic signal, though with significant jitter. **A simple linear fit to our data yields a residual rms scatter of 24.2 m s^{-1} and $\chi^2_{\text{nu}} = 5.23$. By comparison, a planet-only model (no trend) gives an rms of 19.1 m s^{-1} and $\chi^2_{\text{nu}} = 3.65$. We**

fit a planet+trend model, which indicates a planetary companion with $P = 885 \pm 63$ days, $e = 0.03 \pm 0.20$, and $m \sin i = 2.0 \pm 0.5 M_{\text{Jup}}$ (Table 10). That model has a residual rms of 11.0 m s^{-1} and $\chi_{nu}^2 = 1.44$, with a linear trend of $15.4 \pm 6.5 \text{ m s}^{-1} \text{ yr}^{-1}$. Feng et al. (2015) gave a discussion on estimating minimum companion masses from velocity data with such trends when no curvature is evident. Using their Equation 1, which assumes an “unlucky observer” seeing an orbital period $P \sim 1.25 T_{\text{obs}}$ ($= 4.9 \text{ yr}$) and $e \sim 0.5$, we obtain a minimum mass of $2.0 M_{\text{Jup}}$ for the distant outer body. The possibility also exists that the velocity signals of the planet and/or the long-term trend originate from a magnetic activity cycle; however, the velocity amplitudes so induced are less than 10 m s^{-1} (e.g. Robertson et al. 2013, 2015; Fulton et al. 2015).

There remains substantial uncertainty in the fit due to the best-fit 10.65 m s^{-1} velocity jitter for the host star. The residuals to the single planet + trend fit show no coherent periodicity, leading us to conclude that the residual scatter is best explained by stellar noise, as is common for giants (Hekker et al. 2008; Jones et al. 2015). We also note that HD 155233 has a relatively high projected rotational velocity $v \sin i = 4.4 \pm 1.0 \text{ km s}^{-1}$; this is similar to HD 34851 and HD 104358, which have residual scatters of 34.6 m s^{-1} and 15.3 m s^{-1} , respectively (Table 10). The data and model fit are shown in Figure 1.

To check whether the observed velocity variations could be due to intrinsic stellar processes, we examined the All-Sky Automated Survey (ASAS) V band photometric data for HD 155233 (Pojmanski & Maciejewski 2004). A total of 222 epochs were obtained from the ASAS All Star Catalogue¹. After removing 5σ outliers, 218 points remained, and their generalised Lomb-Scargle periodogram (Zechmeister & Kürster 2009) is shown in Figure 2. No periodicities of interest are evident in data spanning 7.4 years. Furthermore, we can use the projected rotational velocity $v \sin i$ and the radius estimate from Table 9 to estimate a maximum rotation period of 58 days, well away from the planetary orbital period of 885 days.

4.2 Four stellar-mass companions

For HD 34851, the rms about the fit is 34.6 m s^{-1} , which is unusually large given that the typical velocity jitter of evolved stars targeted by the PPPS and other surveys is $5\text{--}20 \text{ m s}^{-1}$ (Sato et al. 2005; Johnson et al. 2010a; Jones et al. 2013). The companion has a minimum mass of $345 M_{\text{Jup}}$, or $0.33 M_{\odot}$, corresponding to a mid-M dwarf. The Keplerian orbit fit for HD 34851B and the other three stellar-mass companions are shown in Figure 3.

Nearly two orbital cycles of data result in a well-constrained fit for the massive companion orbiting HD 94386, with an rms of only 5.7 m s^{-1} (Figure 4). The companion has $m \sin i$ of $112.5 M_{\text{Jup}}$ ($= 0.11 M_{\odot}$) corresponding to a late M dwarf. HD 104358 hosts a brown dwarf candidate, with $m \sin i = 69.3 \pm 1.9 M_{\text{Jup}}$ ($= 0.066 M_{\odot}$). The

probability of an inclination small enough to give a stellar-mass companion ($> 80 M_{\text{Jup}}$) is then 50%. The rms about the fit is 15.3 m s^{-1} ; removal of the 4σ outlier at BJD 2455757 gives the same parameters for the companion, though with slightly larger bootstrap uncertainties due to the already-limited amount of data available. Hence we have retained all our data for the fitting. The data and model fit are plotted in Figure 5.

HD 188981 is a known spectroscopic binary (Salzer & Beavers 1985; Pourbaix et al. 2004) that escaped the elimination of binaries in our initial target selection process. Our iodine-cell velocity data have resulted in an extremely precise orbital solution for this system (Table 10 and Figure 6). We obtain $m \sin i = 220.9 M_{\text{Jup}}$ ($= 0.211 M_{\odot}$). Salzer & Beavers (1985) remarked that the host star is ~ 0.1 mag bluer than expected for a solitary K1 giant, and postulated that the stellar companion was an F-type dwarf. An F dwarf companion of $1.2 M_{\odot}$ would require a binary orbital inclination of only $i \sim 10^\circ$. While the spectral lines from such a star would have remained hidden in the data of Salzer & Beavers (1985), the higher resolution and S/N of the AAT data should have produced a double-lined spectrum, which would have caused the planet-search Doppler analysis to fail as for those stars in Table 1. **We simulated the effect of a second light at various levels of contamination. These tests revealed that for a 10% flux contribution from a secondary set of stellar lines, the Doppler code still produces reasonable though somewhat less precise velocities. From Table 9, the luminosity of the primary is $12.3 \pm 0.9 L_{\odot}$, and hence a 10% contamination from the secondary would give $L \lesssim 1.2 L_{\odot}$, corresponding to $\sim 1.05 M_{\odot}$ by the main-sequence mass-luminosity relation. In other words, the lack of a detectable second set of stellar lines at best disfavours very high-mass companions.**

5 DISCUSSION AND CONCLUSIONS

Radial velocity observations of binaries are important in order to determine the masses, arguably the most fundamental parameter of stars. When combined with astrometric observations and parallax measurements, the true masses of the stars can be determined. With the highly anticipated results from the GAIA mission (Perryman et al. 2001), it is important to have radial velocity observations of binary stars in hand as well.

Raghavan et al. (2010) presented a comprehensive study of stellar multiplicity for Sun-like stars in the solar neighbourhood, but their sample did not include evolved stars, and it remains unclear how the orbital parameters of a binary system are affected by a component’s post-main-sequence evolution (but see Veras et al. 2011 and Mustill et al. 2012 for discussion of the effect on planets in such systems). The stellar mass-ratio distribution prefers equal-mass pairs (Raghavan et al. 2010), but none of the four systems presented here has a mass ratio close to unity. However, this is a selection effect, as stars with a mass ratio close to unity would fall into the category of SB2s, which were dropped from this survey. Because suspected binaries were initially avoided in the sample selection (Wittenmyer et al. 2011),

¹ <http://www.astrouw.edu.pl/asas>

any newly discovered binaries will help estimate the number of binaries that have been missed in past estimations of the binary fraction (Duquennoy & Mayor 1991; Raghavan et al. 2010), or verify their incompleteness corrections, respectively. The aforementioned selection biases also make it difficult to compare the binary fraction for evolved stars to that of main sequence stars.

The planet HD 155233b has been independently detected by the EXPRESS survey of M. Jones et al. (2015, in prep). This planet joins the ranks of “typical” planets found to orbit intermediate-mass stars. Such planets are characterised by super-Jupiter masses and semimajor axes beyond ~ 1 AU (Bowler et al. 2010; Johnson et al. 2010b). **For intermediate-mass giants such as HD 155233, giant planet occurrence has been shown to correlate positively with host-star mass (Johnson et al. 2010a). HD 155233 is slightly metal-rich ($[\text{Fe}/\text{H}]=0.10\pm 0.07$), again consistent with the overall trend of increasing giant planet occurrence rate with host-star metallicity (Reffert et al. 2015).**

Hipparcos astrometry has been used for some massive companions to place limits on the system inclination, and hence the true masses (e.g. Kürster et al. 2008; Reffert & Quirrenbach 2011; Wittenmyer et al. 2009a). However, for the stars considered here, the distances are simply too large to make this approach useful at present. Using the distances and the semimajor axes (Table 10), we estimate maximum angular separations as follows: HD 34851B – 0.044 mas; HD 94386B – 0.48 mas; HD 104358B – 0.11 mas; HD 155233b – 0.48 mas; HD 188981B – 0.11 mas. The greater astrometric precision of GAIA, of order 10 micro-arcsec for these bright targets (Perryman et al. 2014), will shed more light on these binary systems.

Since the host stars are old, we are able to investigate whether our newly found large companions are detectable via direct imaging with the latest generation of instruments (GPI & SPHERE) by assuming their luminosities to be similar to that of field main sequence dwarfs. Assuming that the system is edge on (i.e. taking the minimum mass) we could use observed absolute magnitudes as a function of spectral type (collated and plotted in Kirkpatrick et al. 2012) to estimate the contrast ratio of each of our companions and their hosts. By also assuming we are able to observe at the optimal time (maximum projected separation) we use the known distance to the systems to calculate their maximum on-sky separation. We find that although the contrast ratios of these systems are not very large, the very small angular separations cause most of these systems to be inaccessible via direct imaging. Only HD 94386B is potentially detectable via observations using Non-Redundant Masking in conjunction with either SPHERE or GPI. Although HD 155233b’s projected separation is possibly feasible with Non-Redundant Masking, it is a giant planet in an old system, and therefore too faint to be detected with these types of observations (Table 11).

ACKNOWLEDGMENTS

We gratefully acknowledge the efforts of PPPS guest observers Brad Carter, Hugh Jones, and Simon O’Toole. This research has made use of NASA’s Astrophysics Data Sys-

tem (ADS), and the SIMBAD database, operated at CDS, Strasbourg, France. This research has also made use of the Exoplanet Orbit Database and the Exoplanet Data Explorer at exoplanets.org (Wright et al. 2011).

REFERENCES

- Alonso, A., Arribas, S., & Martínez-Roger, C. 1999, *A&A Supplement*, 140, 261
- Alonso, A., Arribas, S., & Martínez-Roger, C. 2001, *A&A*, 376, 1039
- Bailer-Jones, C. A. L. 2011, *MNRAS*, 411, 435
- Bergmann, C., Endl, M., Hearnshaw, J. B., Wittenmyer, R. A., & Wright, D. J. 2015, *International Journal of Astrobiology*, 14, 173
- Bowler, B. P., et al. 2010, *ApJ*, 709, 396
- Butler, R. P., Marcy, G. W., Williams, E., McCarthy, C., Dosanji, P., & Vogt, S. S. 1996, *PASP*, 108, 500
- Campbell, B., Walker, G. A. H., & Yang, S. 1988, *ApJ*, 331, 902
- Castelli, F. & Kurucz, R. L. 2004, *Modelling of Stellar Atmospheres (Proc. IAU Symp. 210)*, ed. N. Piskunov et al. (Dordrecht: Kluwer), poster A20 (arXiv:astro-ph/0405087)
- Diego, F., Charalambous, A., Fish, A. C., & Walker, D. D. 1990, *Proc. Soc. Photo-Opt. Instr. Eng.*, 1235, 562
- Duquennoy, A., & Mayor, M. 1991, *A&A*, 248, 485
- Endl, M., Bergmann, C., Hearnshaw, J., et al. 2015, *International Journal of Astrobiology*, 14, 305
- Feng, Y. K., Wright, J. T., Nelson, B., et al. 2015, *ApJ*, 800, 22
- Fulton, B. J., Weiss, L. M., Sinukoff, E., et al. 2015, *ApJ*, 805, 175
- Grether, D., & Lineweaver, C. H. 2006, *ApJ*, 640, 1051
- Hekker, S., Snellen, I. A. G., Aerts, C., et al. 2008, *Journal of Physics Conference Series*, 118, 012058
- Houk, N., & Smith-Moore, M. 1988, *Michigan Catalogue of Two-dimensional Spectral Types for the HD Stars. Volume 4, Declinations -26.0 to -12.0.*, by N. Houk, M. Smith-Moore. Department of Astronomy, University of Michigan, Ann Arbor, MI 48109-1090, USA. 14+505 pp.
- Houk, N. 1982, *Michigan Catalogue of Two-dimensional Spectral Types for the HD stars. Volume 3. Declinations -40.0 to -26.0.*, by Houk, N.. Ann Arbor, MI(USA): Department of Astronomy, University of Michigan, 12 + 390 p.,
- Houk, N., & Cowley, A. P. 1975, *University of Michigan Catalogue of two-dimensional spectral types for the HD stars. Volume I. Declinations -90 to -53.0.*, by Houk, N.; Cowley, A. P.. Ann Arbor, MI (USA): Department of Astronomy, University of Michigan, 19 + 452 p.,
- Jefferys, W. H., Fitzpatrick, M. J., & McArthur, B. E. 1988, *Celestial Mechanics*, 41, 39
- Johnson, J. A., Aller, K. M., Howard, A. W., & Crepp, J. R. 2010a, *PASP*, 122, 905
- Johnson, J. A., Howard, A. W., Bowler, B. P., Henry, G. W., Marcy, G. W., Wright, J. T., Fischer, D. A., & Isaacson, H. 2010b, *PASP*, 122, 701
- Jones, M. I., Jenkins, J. S., Rojo, P., Melo, C. H. F., & Bluhm, P. 2013, *A&A*, 556, A78

Jones, M. I., Jenkins, J. S., Rojo, P., Melo, C. H. F., & Bluhm, P. 2015, *A&A*, 573, A3

Kirkpatrick, J. D., Gelino, C. R., Cushing, M. C., et al. 2012, *ApJ*, 753, 156

Kürster, M., Endl, M., & Reffert, S. 2008, *A&A*, 483, 869

Marcy, G. W., & Butler, R. P. 2000, *PASP*, 112, 137

Massarotti, A., Latham, D. W., Stefanik, R. P., & Fogel, J. 2008, *AJ*, 135, 209

Mazeh, T., Simon, M., Prato, L., Markus, B., & Zucker, S. 2003, *ApJ*, 599, 1344

McDonald, I., Zijlstra, A. A., & Boyer, M. L. 2012, *MNRAS*, 427, 343

Meschiari, S., Wolf, A. S., Rivera, E., et al. 2009, *PASP*, 121, 1016

Murdoch, K. A., Hearnshaw, J. B., & Clark, M. 1993, *ApJ*, 413, 349

Mustill, A. J., & Villaver, E. 2012, *ApJ*, 761, 121

Patel, S. G., Vogt, S. S., Marcy, G. W., et al. 2007, *ApJ*, 665, 744

Perryman, M. A. C., et al. 1997, *A&A*, 323, L49

Perryman, M. A. C., de Boer, K. S., Gilmore, G., et al. 2001, *A&A*, 369, 339

Perryman, M., Hartman, J., Bakos, G. Á., & Lindegren, L. 2014, *ApJ*, 797, 14

Pojmanski, G., & Maciejewski, G. 2004, *Acta Astronomica*, 54, 153

Pourbaix, D., Tokovinin, A. A., Batten, A. H., et al. 2004, *A&A*, 424, 727

Raghavan, D., McAlister, H. A., Henry, T. J., et al. 2010, *ApJS*, 190, 1

Randich, S., Gratton, R., Pallavicini, R., Pasquini, L., & Carretta, E. 1999, *A&A*, 348, 487

Reffert, S., & Quirrenbach, A. 2011, *A&A*, 527, A140

Reffert, S., Bergmann, C., Quirrenbach, A., Trifonov, T., Kunstler, A. 2015, *A&A*, 574, A116

Robertson, P., Endl, M., Cochran, W. D., MacQueen, P. J., & Boss, A. P. 2013, *ApJ*, 774, 147

Robertson, P., Endl, M., Henry, G. W., et al. 2015, *ApJ*, 801, 79

Salzer, J. J., & Beavers, W. I. 1985, *PASP*, 97, 637

Sato, B., Kambe, E., Takeda, Y., et al. 2005, *PASJ*, 57, 97

Schlegel, D. J., Finkbeiner, D. P., & Davis, M. 1998, *ApJ*, 500, 525

Swift, J. 2015, *Journal of Astronomical Telescopes, Instruments, and Systems*, 1, 027002

Tinney, C. G., Wittenmyer, R. A., Butler, R. P., et al. 2011, *ApJ*, 732, 31

Valenti, J. A., Butler, R. P. & Marcy, G. W. 1995, *PASP*, 107, 966.

van Leeuwen, F. 2007, *A&A*, 474, 653

Veras, D., Wyatt, M. C., Mustill, A. J., Bonsor, A., & Eldridge, J. J. 2011, *MNRAS*, 417, 2104

Wittenmyer, R. A., Endl, M., Cochran, W. D., et al. 2009a, *AJ*, 137, 3529

Wittenmyer, R. A., Endl, M., Cochran, W. D., Levison, H. F., & Henry, G. W. 2009b, *ApJS*, 182, 97

Wittenmyer, R. A., Endl, M., Wang, L., et al. 2011, *ApJ*, 743, 184

Wittenmyer, R. A., Wang, L., Liu, F., et al. 2015, *ApJ*, 800, 74

Wright, J. T., Fakhouri, O., Marcy, G. W., et al. 2011, *PASP*, 123, 412

Table 1. Double-lined spectroscopic binaries in the PPPS sample

HD	HIP
749	944
5873	4696
5877	4618
20035	14868
31860	23061
46122	31118
58540	35790
76321	43772
81410	46159
98579	55374
136905	73525
137164	75689
142384	78027
153438	83224
176650	93383
176794	94208
204203	105953

Table 2. Summary of observations

Star	N_{obs}	Span (days)	Mean uncertainty (m s^{-1})
HD 34851	9	1278	6.0
HD 47205	27	1881	1.1
HD 94386	14	1512	1.8
HD 104358	12	1880	2.7
HD 155233	21	1426	2.1
HD 188981	16	1453	2.3

Yi, S. K., Kim, Y.-C., & Demarque, P. 2003, *ApJS*, 144, 259

Zechmeister, M., Kürster, M. 2009, *A&A*, 496, 577

Table 3. AAT radial velocities for HD 34851

BJD-2400000	Velocity (m s^{-1})	Uncertainty (m s^{-1})
55251.94376	1418.0	3.6
55525.13661	-15566.3	7.3
55580.07072	-12641.7	6.8
55602.00949	334.7	3.5
55879.17147	-1270.4	6.7
55906.06875	-8285.2	6.2
55969.98892	-6009.1	6.8
56375.89323	0.0	6.4
56529.27818	-8020.4	6.4

Table 4. AAT radial velocities for HD 47205

BJD-2400000	Velocity (m s^{-1})	Uncertainty (m s^{-1})
54866.09965	28.1	0.8
54866.94000	18.4	1.3
54867.91576	26.6	1.3
54869.08575	20.8	1.0
54871.03478	30.4	1.3
55140.18899	-29.1	0.9
55227.06602	-18.4	1.3
55317.85835	0.8	0.6
55525.22369	34.4	1.4
55526.21028	38.8	0.9
55581.09317	43.3	1.1
55601.00002	36.9	0.9
55706.84304	-5.3	1.0
55783.30462	-25.6	1.0
55879.26442	-46.9	1.1
55880.21953	-38.9	0.9
55906.04456	-38.4	1.1
55969.96686	-37.2	0.8
55994.95994	-20.4	0.9
56051.86418	1.6	1.4
56059.86471	-4.0	1.6
56343.99185	47.7	0.9
56374.88203	55.7	1.2
56377.97935	54.8	0.9
56526.27125	-4.2	1.0
56685.97593	-27.9	0.9
56747.92127	-22.7	1.3

Table 5. AAT radial velocities for HD 94386

BJD-2400000	Velocity (m s^{-1})	Uncertainty (m s^{-1})
54866.16823	-1122.3	1.5
55227.08417	386.9	1.2
55380.83884	2145.4	1.2
55580.16602	490.7	2.0
55601.19789	15.7	1.8
55602.15229	-4.4	1.6
55706.90383	-1032.6	1.3
55970.13115	-664.4	1.1
55994.09656	-556.4	2.6
56059.90490	-237.2	2.5
56088.91084	-69.2	1.9
56345.09758	2755.5	2.6
56375.98219	3125.8	1.6
56378.02772	3162.6	1.6

Table 6. AAT radial velocities for HD 104358

BJD-2400000	Velocity (m s^{-1})	Uncertainty (m s^{-1})
54867.22642	-2349.3	2.0
55706.89202	-2436.0	1.9
55757.87488	-745.0	5.4
55970.17721	-2479.1	1.9
55994.10810	-2265.1	4.2
56059.94668	-66.3	2.9
56086.95956	543.4	2.2
56088.92816	596.7	2.2
56344.12214	0.0	3.7
56377.03081	683.3	2.4
56378.03502	708.8	2.3
56747.00059	609.4	2.0

Table 7. AAT radial velocities for HD 155233

BJD-2400000	Velocity (m s^{-1})	Uncertainty (m s^{-1})
55319.20751	-76.0	2.1
55382.09355	-68.9	1.6
55602.27053	-10.5	2.8
55707.20272	12.8	1.8
55757.95688	3.4	2.5
55760.09094	24.8	2.0
55841.92832	11.7	2.9
55970.27601	-12.2	1.4
55994.24764	9.4	2.1
56052.14878	-48.3	2.4
56089.07696	-16.1	1.8
56134.99850	-29.0	1.9
56344.27771	-12.7	1.6
56375.25095	-0.2	2.4
56376.23958	11.5	1.6
56400.13392	-3.8	1.6
56470.07735	2.9	3.8
56494.98115	22.1	1.6
56525.93237	37.0	1.8
56529.98008	18.1	2.3
56745.23184	47.2	1.2

Table 8. AAT radial velocities for HD 188981

BJD-2400000	Velocity (m s^{-1})	Uncertainty (m s^{-1})
55074.06452	-399.2	1.9
55318.32115	-8926.5	2.5
55455.97154	7190.8	1.9
55670.31992	0.0	1.4
55707.29018	6601.1	1.5
55760.04921	-8824.9	6.1
55842.90819	6847.6	2.0
55994.29530	-3545.9	2.2
56052.20653	-1600.1	1.7
56060.24069	-4710.4	3.0
56089.16329	8535.9	1.6
56469.14010	8110.5	2.7
56470.23672	7760.3	2.0
56494.06543	-2017.2	1.7
56495.07148	-2425.4	1.8
56527.06483	7795.5	2.1

Table 9. Stellar Parameters for Host Stars

Parameter	HD 34851		HD 94386		HD 104358		HD 155233		HD 188981	
	Value	Ref.	Value	Ref.	Value	Ref.	Value	Ref.	Value	Ref.
Spec. Type	K2 III	2	K3 IV	7	K0 III	8	K1 III	8	K1 III	10
	K2 III	8								
$(B - V)$	1.095	3	1.176	3	1.136	3	1.030±0.008	4	1.051	3
$E(B - V)$	0.0436		0.0189		0.0367		0.0338		0.0232	
A_V	0.1359		0.0590		0.1146		0.106		0.0724	
Mass (M_\odot)	2.00±0.22	1	1.19±0.19	1	1.27±0.21	1	1.50±0.20	1	1.49±0.20	1
	1.1	7	1.1	7						
Distance (pc)	161.6±12.5	4	73.8±4.7	4	150.2±15.8	4	75.1±3.3	4	58.9±2.2	4
$V \sin i$ (km s^{-1})	4.6±0.9	1	<1	1	4.1±0.5	1	4.4±1.0	1	<1	1
	<1	7	<1	7						
$[Fe/H]$	0.29±0.14	1	0.19±0.10	1	0.06±0.08	1	0.10±0.07	1	0.18±0.07	1
	0.08±0.09	7	0.08±0.09	7	0.08±0.09	7				
T_{eff} (K)	4787±100	1	4558±100	1	4631±100	1	4845±100	1	4802±100	1
	4815	5	4436±13	9	4400	5	4436±13	9	4436±13	9
	4804±200	6	4545±42	7	4656±200	6	4545±42	7	4545±42	7
$\log g$	3.05±0.09	1	2.80±0.10	1	2.80±0.12	1	3.21±0.08	1	3.20±0.08	1
	2.7	9	2.7	9	2.7	9				
	2.7±0.3	7	2.7±0.3	7	2.7±0.3	7				
Luminosity (L_\odot)	23.1±3.6	1	20.1±2.6	1	22.7±4.8	1	12.5±1.1	1	12.3±0.9	1
Radius (R_\odot)	7.0±0.6	1	7.2±0.6	1	7.4±0.8	1	5.03±0.22	1	5.0±0.3	1

Refernces: 1 - This work, 2 - Houk & Cowley (1975), 3 - Perryman et al. (1997), 4 - van Leeuwen (2007), 5 - McDonald et al. (2012), 6 - Bailer-Jones (2011), 7 - Randich et al. (1999), 8 - Houk & Smith-Moore (1988), 9 - Massarotti et al. (2008), 10 - Houk (1982),

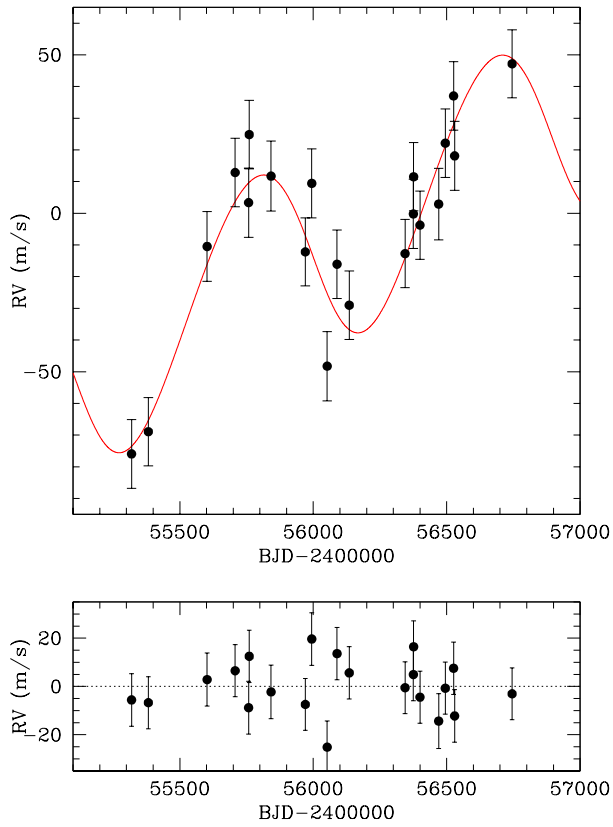


Figure 1. Top panel: AAT data and Keplerian fit for a $2M_{\text{Jup}}$ planet orbiting HD 155233. A linear trend of $15.4 \pm 6.5 \text{ m s}^{-1} \text{ yr}^{-1}$ is included in the fit as a free parameter and is shown. Error bars include 10.65 m s^{-1} of jitter added in quadrature. The rms about this fit is 10.9 m s^{-1} ; residuals are shown in the bottom panel.

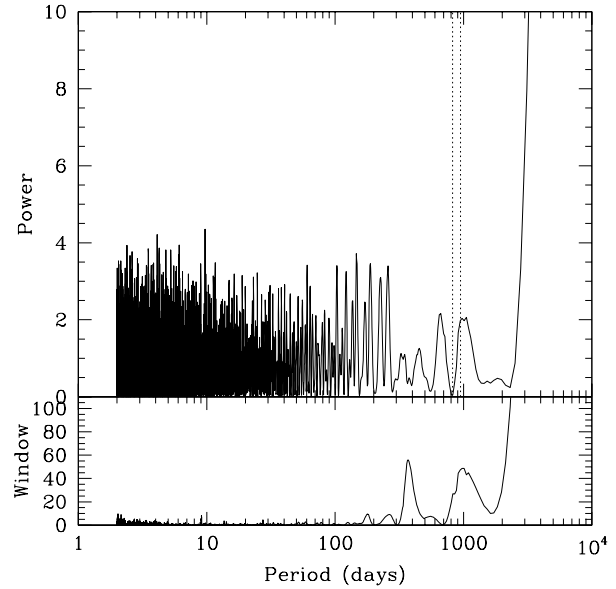


Figure 2. Generalised Lomb-Scargle periodogram of ASAS photometry for HD 155233. A total of 218 epochs spanning 7.4 years yield no significant periodicities. The $\pm 1\sigma$ range of the planet's orbital period is shown as vertical dashed lines ($885 \pm 63 \text{ d}$).

Table 10. New and updated Keplerian orbital solutions

Parameter	HD 34851B	HD 47205 b	HD 94386 B	HD 104358 B	HD 155233 b	HD 188981 B
Period (days)	62.304±0.005	796.0±7.4	925.0±1.0	281.1±0.3	885±63	62.9637±0.0008
T_0 (BJD-2400000)	55214.7±0.4	54093±34	54582.1±1.2	54836.8±4.2	55112±412	55011.487±0.008
Eccentricity	0.21±0.01	0.22±0.07	0.422±0.004	0.24±0.02	0.03±0.20	0.4218±0.0007
ω (degrees)	203±2	77±14	37.8±0.2	146±7	95±90	274.60±0.06
K (m s^{-1})	10296±144	41.8±2.4	2176±12	1828±42	32.2±8.7	8735.6±2.2
$m \sin i$ (M_{Jup})	345.4±5.4	2.46±0.14	112.5±0.5	69.3±1.9	2.0±0.5	220.90±0.08
a (AU)	0.4078±0.0003	1.93±0.01	2.0266±0.0015	0.9251±0.0007	2.07±0.10	0.369753±0.000005
RMS about fit (m s^{-1})	34.6	6.5	5.7	15.3	10.9	5.3

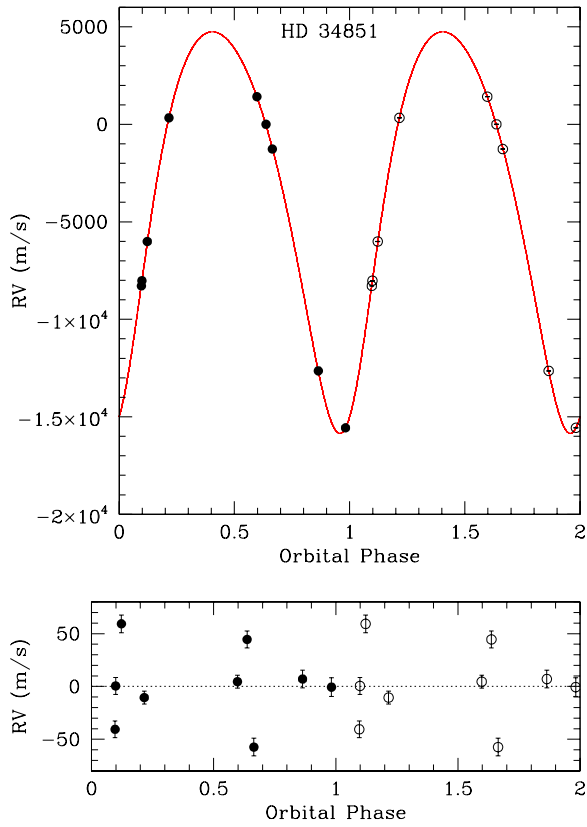


Figure 3. AAT radial velocity data and Keplerian orbit fit for HD 34851B (top) and residuals to the fit (bottom). The data are phase-folded and two cycles are shown for clarity.

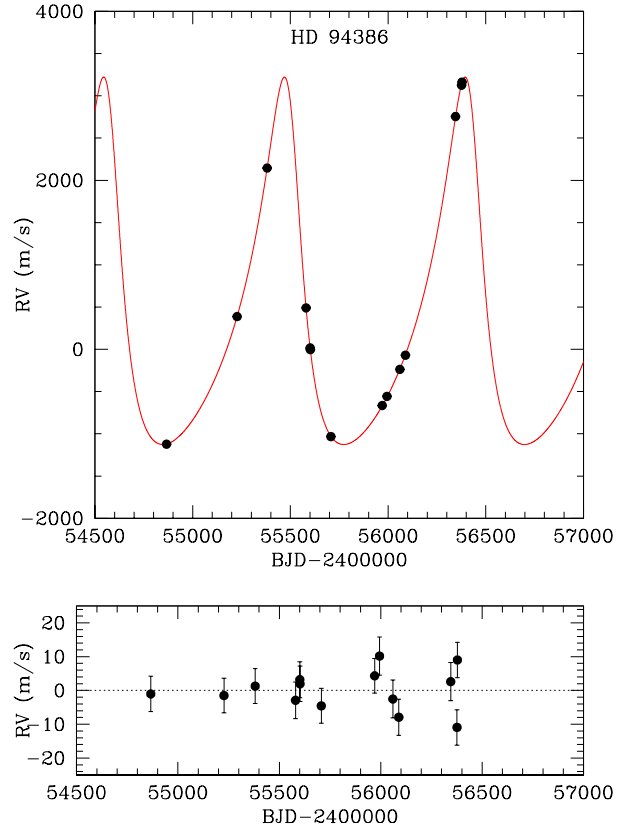


Figure 4. AAT radial velocity data and Keplerian orbit fit for HD 94386B (top) and residuals to the fit (bottom).

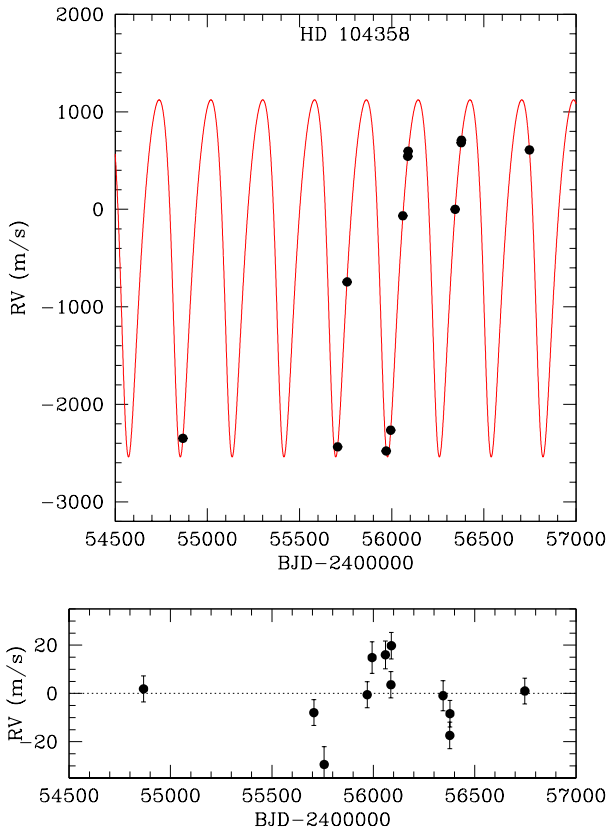


Figure 5. AAT radial velocity data and Keplerian orbit fit for HD 104358B (top) and residuals to the fit (bottom).

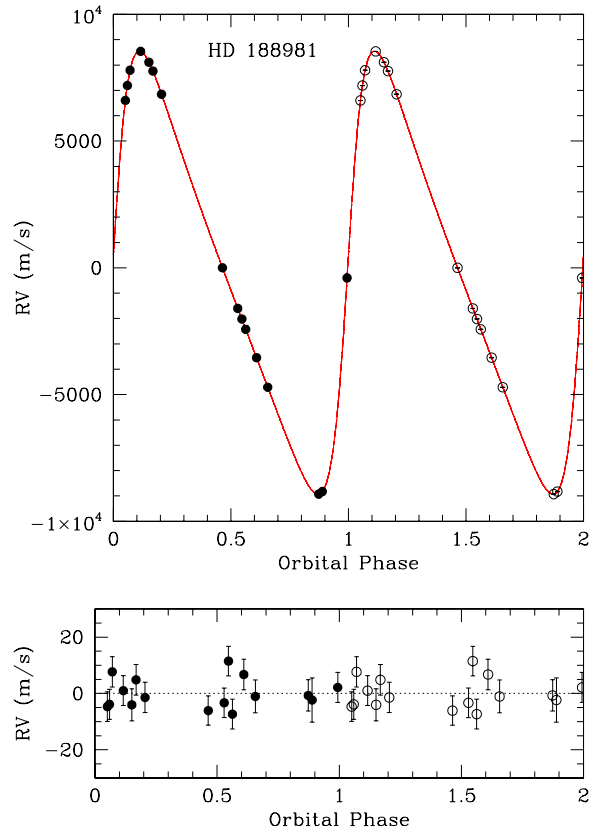


Figure 6. AAT radial velocity data and Keplerian orbit fit for HD 188981B (top) and residuals to the fit (bottom). The data are phase-folded and two cycles are shown for clarity.

Table 11. Estimated contrast ratios. Companion masses are assumed to be the minimum $m \sin i$ as given in Table 10, and separations are taken to be the maximum for each object modulo its orbital eccentricity and semimajor axis.

Host	SpT	Companion mass (M_{\odot})	SpT-companion	Separation (AU)	Distance (pc)	Contrast (mag)	On-sky separation (mas)
HD 34851B	K2 III	> 0.33	<M4	< 0.49	161.6	< 3.9	< 3
HD 94386B	K3 III	> 0.11	<M8/L0	< 2.88	73.8	< 5.3	< 39
HD 104358B	K0 III	> 0.066	<L5	< 1.147	150.2	< 7.4	< 7.6
HD 188981B	K1 III	> 0.211	<M6	< 0.52	58.9	< 5.0	< 8.8
HD 155233b	K1 III	> 2.13	>2.0 M_{Jup}	< 2.13	75.1	...	< 28.3